Int. J. Electron. Commun. (AEÜ) 66 (2012) 687–692

Contents lists available at SciVerse ScienceDirect

International Journal of Electronics and Communications (AEÜ)

journal homepage: www.elsevier.de/aeue

Estimation of highly selective channels for OFDM system by complex least squares support vector machines

Anis Charrada, Abdelaziz Samet

Tunisia Polytechnic School, University of Carthage, Box 743, La Marsa 2078, Tunisia

ARTICLE INFO

Article history:
Received 3 May 2011
Accepted 16 December 2011

Keywords:
Complex SVM
LS-SVM
Mercer's kernel
Channel estimation
OFDM
LTE

ABSTRACT

A channel estimator using complex least squares support vector machines (LS-SVM) is proposed for pilot-aided OFDM system and applied to Long Term Evolution (LTE) downlink. This channel estimation algorithm use knowledge of the pilot signals to estimate the total frequency response of the channel. Thus, the algorithm maps trained data into a high dimensional feature space and uses the structural risk minimization (SRM) principle, which minimizes an upper bound on the generalization error, to carry out the regression estimation for the frequency response function of the highly selective channel. Simulation results show that the proposed method has better performance compared to the conventional LS and Decision Feedback methods and it is more robust at high speed mobility.

1. Introduction

Support vector machines (SVMs) have shown several advantages in regression, prediction and estimation over some of the classical approaches due to its improved generalization capabilities. Here, a proposed SVM robust version for channel estimation that is specifically adapted to pilot-aided OFDM (Orthogonal Frequency Division Multiplexing) structure is presented. In fact, the channel estimation algorithm is based on the complex least squares support vector machines (LS-SVM) method in order to improve communication efficiency and quality of OFDM systems. The principle of the proposed nonlinear complex LS-SVM algorithm is to exploit the information provided by the reference signal to estimate the channel frequency response. In highly selective multipath fading channel, where complicated nonlinearities can be present, the estimation precision can be lowed by using linear method. So, we adapt the nonlinear complex LS-SVM algorithm which transforms the nonlinear estimation in low dimensional space into the linear estimation in high dimensional space improving thus the estimation precision.

In this contribution, the proposed nonlinear complex LS-SVM technique is developed and applied to LTE (Long Term Evolution) downlink highly selective channel using pilot symbols. For the purpose of comparison with conventional algorithms such that LS and Decision Feedback, we develop the nonlinear complex LS-SVM algorithm in terms of the RBF (Radial Basis Function) kernel. Two scenarios in simulation section illustrate the advantage of this algorithm over LS and Decision Feedback algorithms and compare the behavior of these algorithms in high mobility environments. The nonlinear complex LS-SVM method shows good results in two scenarios of mobility variations due to its improved generalization ability.

The scheme of the paper is as follows. We present a related work in Section 2. Section 3 briefly introduces the OFDM system model. Then, we present LS and Decision Feedback channel estimation methods with the formulation of the proposed nonlinear complex LS-SVM method in Section 4. Section 5 shows the simulation results when comparing with LS and Decision Feedback algorithms. Finally, in Section 6, conclusions are given.

2. Related work

The use of SVM has already been proposed to solve a variety of signal processing and digital communications problems, such that channel estimation by linear SVM in OFDM system which is presented in [1]. This study is specifically adapted to a pilots-based OFDM signal in a flat-fading channel and uses the block-type pilot structure. In this type, pilot tones are inserted into all subcarriers of pilot symbols with a period in time for channel estimation. This block-type pilot arrangement is suitable for slow fading channels. In fact, [1] consider a packet-based transmission, where each packet consists of a header at the beginning of the packet with a known training sequence or preamble to carry out channel estimation, followed by a certain number of OFDM data symbols. At the preamble,

E-mail address: anis.charrada@gmail.com (A. Charrada).

1434-8411/$ – see front matter © 2012 Elsevier GmbH. All rights reserved.
doi:10.1016/j.aeue.2011.12.011

there are a number of OFDM symbols with a fixed number of pilot subcarriers in order to estimate the channels coefficient at pilot positions and then perform interpolation of the channel over all the OFDM symbols in the packet.

However, in fast-fading channels, block-type pilot arrangement is not efficient and comb-type pilot arrangement is suitable especially in high mobility environments.

On the other hand, in [1], the channel's frequency response is estimated over a subset of pilot subcarriers and then interpolated over the remaining (data) subcarriers by using a DFT (Discret Fourier Transform) based technique with zero padding in the time domain. Therefore, the learning process can be more complex if the size of the pilot symbols is large, so the estimation task becomes slow.

The work of our paper focus on the nonlinear SVM applied to an OFDM system under high mobility conditions with comb-type pilot structure for fast fading channel. The OFDM system under consideration requires an estimate of the frequency responses of data subchannels for each OFDM symbol. Therefore, the learning and estimation phases are repeated for each OFDM symbol in order to track the channel variation. The use of the nonlinear SVM approach is needed for the channel estimation in deep fading environment. Indeed, Mercer's theorem announced that $\mathbf{x}$ in a finite dimension space (input space) can be mapped to a higher dimensional Hilbert space provided with a dot product through a nonlinear transformation $\boldsymbol{\varphi}(\cdot)$. Thus, a linear machine can be constructed in a higher dimensional space (feature space), but it stays nonlinear in the input space. Note that most of the transformations $\boldsymbol{\varphi}(\cdot)$ are unknown, but the dot product of the corresponding spaces can be expressed as a function of the input vectors as

$$\mathbf{K}(\mathbf{x}_i, \mathbf{x}_j) = \langle \boldsymbol{\varphi}(\mathbf{x}_i), \boldsymbol{\varphi}(\mathbf{x}_j)\rangle. \tag{1}$$

These spaces are called Reproducing Kernel Hilbert Spaces (RKHS), and their dot products $\mathbf{K}(\mathbf{x}_i, \mathbf{x}_j)$ are called Mercer kernels. Thus, it is possible to explicitly represent an SVM into a Hilbert spaces. The Mercer's theorem gives the condition that a kernel $\mathbf{K}(\mathbf{x}_i, \mathbf{x}_j)$ must satisfy in order to be the dot product of a Hilbert space. The most popular kernel which satisfy Mercer's conditions is the RBF (Gaussian kernel) which is expressed as

$$\mathbf{K}(\mathbf{x}_i, \mathbf{x}_j) = \exp - \frac{\|\mathbf{x}_i - \mathbf{x}_j\|^2}{2\sigma^2}. \tag{2}$$

In this contribution, moreover, we use the indices of pilot positions (as input in training phase) to estimate the channel frequency responses at these pilot positions (as output in training phase), and then channel frequency responses at all subcarriers in each OFDM symbol can be obtained by SVM interpolation.

3. System model

The discret-time received signal for the OFDM system comprising N subcarriers can be expressed as

$$y(n) = \sum_{k \in \Omega_P} X^P(k) H(k) \exp\left(j\frac{2\pi}{N}kn\right) + \sum_{k \notin \Omega_P} X^D(k) H(k) \exp\left(j\frac{2\pi}{N}kn\right) + w_g(n) \tag{3}$$

where Ω_P is the subset of N_P pilot subcarriers, $X^P(k)$ and $X^D(k)$ are complex pilot and data symbol respectively, transmitted at the kth frequency, $H(k) = DFT_N\{h(n)\}$ is the channel's frequency response at the kth subcarrier and $w_g(n)$ is a complex white Gaussian noise process $N(0, \sigma_w^2)$ with power spectral density $N_0/2$. It is well known that if the channel impulse response has a maximum of L resolvable paths, then the guard interval must be at least equal to L [2].

After DFT transformation, assuming that ISI (Inter Symbol Interference) are eliminated, $y(n)$ becomes

$$Y(k) = X(k)H(k) + W_G(k). \tag{4}$$

Equation (4) may be presented in matrix notation

$$Y = \mathbf{XF}h + W_G = \mathbf{X}H + W_G \tag{5}$$

where

$$\mathbf{X} = diag(X(0), X(1), \ldots, X(N-1))$$
$$Y = [Y(0), \ldots, Y(N-1)]^T$$
$$W_G = [W_G(0), \ldots, W_G(N-1)]^T$$
$$H = [H(0), \ldots, H(N-1)]^T$$
$$\mathbf{F} = \begin{bmatrix} {F_N}^{00} & \cdots & {F_N}^{0(N-1)} \\ {F_N}^{10} & \cdots & {F_N}^{1(N-1)} \\ \vdots & \ddots & \vdots \\ {F_N}^{(N-1)0} & \cdots & {F_N}^{(N-1)(N-1)} \end{bmatrix} \text{ and } F_N^{i,k} = \left(\frac{1}{\sqrt{N}}\right) \exp\left(-j2\pi\left(\frac{ik}{N}\right)\right). \tag{6}$$

4. Channel estimation

4.1. Least squares channel estimation

The principal of the channel least squares estimator is minimizing the square distance between the received signal Y and the original signal X as follows:

$$\min_{H^\dagger} J(H) = \min_{H^\dagger}\{|Y - XH|^2\} = \min_{H^\dagger}\{(Y - XH)^\dagger (Y - XH)\} \tag{7}$$

where, $(\cdot)^\dagger$ is the conjugate transpose operator. By differentiating (7) with respect to $H^\dagger$ and finding the minima, we obtain the LS channel estimation which is given by

$$\hat{H}_{LS} = X^{-1}Y. \tag{8}$$

4.2. Estimation with Decision Feedback

OFDM channel estimation with Decision Feedback uses the reference symbols to estimate the channel response using LS algorithm. For each coming symbol i and for each subcarrier k for $k = 0, \ldots, N-1$, the estimated transmitted symbol is found from the previous $H(i, k)$ according to the formula

$$\hat{X}(i+1, k) = \frac{Y(i+1, k)}{\widehat{H}(i, k)} \tag{9}$$

The estimated received symbols $\hat{X}(i+1, k)$ are used to make the decision about the real transmitted symbol values $\tilde{X}(i+1, k)$. The estimated channel response is updated by

$$\hat{H}(i+1, k) = \frac{Y(i+1, k)}{\tilde{X}(i+1, k)} \tag{10}$$

Therefore, $\hat{H}(i+1, k)$ is used as a reference in the next symbol for the channel equalization.

4.3. Complex LS-SVM estimator

First, let the OFDM frame contains Ns OFDM symbols which every symbol includes N subcarriers. The transmitting pilot symbols are $\mathbf{X}^P = diag(X(i, m\Delta P))$, $m = 0, 1, \ldots, N_P - 1$, where i and m are labels in time domain and frequency domain respectively, and ΔP is the pilot interval in frequency domain. Note that, pilot insertion in the subcarriers of every OFDM symbol must satisfy the demand of the sampling theory and uniform distribution [3].

The proposed channel estimation method is based on complex LS-SVM algorithm which has two separate phases: training phase and estimation phase. In training phase, we estimate first the subchannels pilot symbols according to LS criterion to strike $\min[(Y^P - \mathbf{X}^P\mathbf{F}h)(Y^P - \mathbf{X}^P\mathbf{F}h)^H]$ [4], as

$$\widehat{H}^P = \mathbf{X}^{P^{-1}} Y^P \tag{11}$$

where $Y^P = Y(i, m\Delta P)$ and $\widehat{H}^P = \widehat{H}(i, m\Delta P)$ are the received pilot symbols and the estimated frequency responses for the ith OFDM symbol at pilot positions $m\Delta P$, respectively.

Then, in the estimation phase and by the interpolation mechanism, frequency responses of data subchannels can be determined. Therefore, frequency responses of all the OFDM subcarriers are

$$\widehat{H}(i, q) = f(\widehat{H}^P(i, m\Delta P)) \tag{12}$$

where $q = 0, \ldots, N-1$, and $f(\cdot)$ is the interpolating function, which is determined by the nonlinear complex LS-SVM approach.

In high mobility environments, where the fading channels present very complicated nonlinearity especially in deep fading case, the linear approaches cannot achieve high estimation precision. Therefore, we adapt here a nonlinear complex LS-SVM technique since SVM is superior in solving nonlinear, small samples and high dimensional pattern recognition [3]. Therefore, we map the input vectors to a higher dimensional feature space $\mathcal{H}$ (possibly infinity) by means of nonlinear transformation $\boldsymbol{\varphi}$. Thus, the regularization term is referred to the regression vector in the RKHS. The following linear regression function is then

$$\widehat{H}(m\Delta P) = \mathbf{w}^T\boldsymbol{\varphi}(m\Delta P) + b + e_m, \quad m = 0, \ldots, N_P - 1 \tag{13}$$

where $\mathbf{w}$ is the weight vector, b is the bias term well known in the SVM literature and residuals $\{e_m\}$ account for the effect of both approximation errors and noise. In the SVM framework, the optimality criterion is a regularized and constrained version of the regularized LS criterion. In general, SVM algorithms minimize a regularized cost function of the residuals, usually the Vapnik's ε-insensitivity cost function [5].

A robust cost function is introduced to improve the performance of the estimation algorithm which is ε-Huber robust cost function [6], given by

$$\mathcal{L}^{\varepsilon}(e_m) = \begin{cases} 0, & |e_m| \le \varepsilon \\ \dfrac{1}{2\gamma}(|e_m| - \varepsilon)^2, & \varepsilon \le |e_m| \le e_C \\ C(|e_m| - \varepsilon) - \dfrac{1}{2}\gamma C^2, & e_C \le |e_m| \end{cases} \tag{14}$$

where $e_C = \varepsilon + \gamma C$, ε is the insensitive parameter which is positive scalar that represents the insensitivity to a low noise level, parameters γ and C control essentially the trade-off between the regularization and the losses, and represent the relevance of the residuals that are in the linear or in the quadratic cost zone, respectively. The cost function is linear for errors above e_C, and quadratic for errors between ε and e_C. Note that, errors lower than ε are ignored in the ε-insensitivity zone. On the other hand, the quadratic cost zone uses the L_2-*norm* of errors, which is appropriate for Gaussian noise, and the linear cost zone limits the effect of sub-Gaussian noise [1]. Therefore, the ε-Huber robust cost function can be adapted to different kinds of noise.

Let $\mathcal{L}^{\varepsilon}(e_m) = \mathcal{L}^{\varepsilon}(\Re(e_m)) + \mathcal{L}^{\varepsilon}(\Im(e_m))$ since $\{e_m\}$ are complex, where $\Re(\cdot)$ and $\Im(\cdot)$ represent real and imaginary parts, respectively. Now, we can state the primal problem as minimizing

$$\frac{1}{2}\|\mathbf{w}\|^2 + \frac{1}{2\gamma}\sum_{m\in I_1}(\xi_m + \xi_m^*)^2 + C\sum_{m\in I_2}(\xi_m + \xi_m^*) + \frac{1}{2\gamma}\sum_{m\in I_3}(\zeta_m + \zeta_m^*)^2 + C\sum_{m\in I_4}(\zeta_m + \zeta_m^*) - \frac{1}{2}\sum_{m\in I_2, I_4}\gamma C^2 \tag{15}$$

constrained to

$$\begin{aligned} &\Re(\hat{H}(m\Delta P) - \mathbf{w}^T\boldsymbol{\varphi}(m\Delta P) - b) \le \varepsilon + \xi_m \\ &\Im(\hat{H}(m\Delta P) - \mathbf{w}^T\boldsymbol{\varphi}(m\Delta P) - b) \le \varepsilon + \zeta_m \\ &\Re(-\hat{H}(m\Delta P) + \mathbf{w}^T\boldsymbol{\varphi}(m\Delta P) + b) \le \varepsilon + \xi_m^* \\ &\Im(-\hat{H}(m\Delta P) + \mathbf{w}^T\boldsymbol{\varphi}(m\Delta P) + b) \le \varepsilon + \zeta_m^* \\ &\xi_m^{(*)}, \zeta_m^{(*)} \ge 0 \end{aligned} \tag{16}$$

for $m = 0, \ldots, N_P - 1$, where ξ_m and ξ_m^* are slack variables which stand for positive, and negative errors in the real part, respectively. ζ_m and ζ_m^* are the errors for the imaginary parts. I_1, I_2, I_3 and I_4 are the set of samples for which:

I_1: real part of the residuals are in the quadratic zone;
I_2: real part of the residuals are in the linear zone;
I_3: imaginary part of the residuals are in the quadratic zone;
I_4: imaginary part of the residuals are in the linear zone.

To transform the minimization of the primal functional (15) subject to constraints in (16), into the optimization of the dual functional, we must first introduce the constraints into the primal functional to obtain the primal–dual functional as follow:

$$\begin{aligned} L_{Pd} = {}& \frac{1}{2}\|\mathbf{w}\|^2 + \frac{1}{2\gamma}\sum_{m\in I_1}(\xi_m + \xi_m^*)^2 + C\sum_{m\in I_2}(\xi_m + \xi_m^*) \\ &+ \frac{1}{2\gamma}\sum_{m\in I_3}(\zeta_m + \zeta_m^*)^2 + C\sum_{m\in I_4}(\zeta_m + \zeta_m^*) - \frac{1}{2}\sum_{m\in I_2, I_4}\gamma C^2 \\ &- \sum_{m=0}^{N_{P-1}}(\beta_m\xi_m + \beta_m^*\xi_m^*) - \sum_{m=0}^{N_{P-1}}(\lambda_m\zeta_m + \lambda_m^*\zeta_m^*) \\ &+ \sum_{m=0}^{N_{P-1}}\alpha_{R,m}[\Re(\widehat{H}(m\Delta P) - \mathbf{w}^T\boldsymbol{\varphi}(m\Delta P) - b) - \varepsilon - \xi_m] \\ &+ \sum_{m=0}^{N_{P-1}}\alpha_{I,m}[\Im(\widehat{H}(m\Delta P) - \mathbf{w}^T\boldsymbol{\varphi}(m\Delta P) - b) - j\varepsilon - j\zeta_m] \\ &+ \sum_{m=0}^{N_{P-1}}\alpha_{R,m}^*[\Re(-\widehat{H}(m\Delta P) + \mathbf{w}^T\boldsymbol{\varphi}(m\Delta P) + b) - \varepsilon - \xi_m^*] \\ &+ \sum_{m=0}^{N_{P-1}}\alpha_{I,m}^*[\Im(-\widehat{H}(m\Delta P) + \mathbf{w}^T\boldsymbol{\varphi}(m\Delta P) + b) - j\varepsilon - j\zeta_m^*] \end{aligned} \tag{17}$$

with the Lagrange multipliers (or dual variables) constrained to $\alpha_{R,m}, \alpha_{I,m}, \beta_m, \lambda_m, \alpha_{R,m}^*, \alpha_{I,m}^*, \beta_m^*, \lambda_m^* \ge 0$ and $\xi_m, \zeta_m, \xi_m^*, \zeta_m^* \ge 0$.

According to Karush–Kuhn–Tucker (KKT) conditions [6]

$$\beta_m\xi_m = 0, \quad \beta_m^*\xi_m^* = 0 \quad \text{and} \quad \lambda_m\zeta_m = 0, \quad \lambda_m^*\zeta_m^* = 0. \tag{18}$$

Then, by making zero the primal–dual functional gradient with respect to ω_i, we obtain an optimal solution for the weights

$$\mathbf{w} = \sum_{m=0}^{N_P-1}\psi_m\boldsymbol{\varphi}(m\Delta P) = \sum_{m=0}^{N_P-1}\psi_m\boldsymbol{\varphi}(P_m) \tag{19}$$

Table 1
Extended vehicular A model (EVA) [7].

Excess tap delay [ns]	Relative power [dB]
0	.0
30	−1.5
150	−1.4
310	−3.6
370	−.6
710	−9.1
1090	−7.0
1730	−12.0
2510	−16.9

Table 2
Parameters of simulations [8–10].

Parameters	Specifications
OFDM system	LTE/Downlink
Constellation	16-QAM
Mobile speed (km/h)	120/350
T_s (μs)	72
f_c (GHz)	2.15
δf (kHz)	15
B (MHz)	5
Size of DFT/IDFT	512
Number of paths	9

where $\psi_m = (\alpha_{R,m} - \alpha^*_{R,m}) + j(\alpha_{I,m} - \alpha^*_{I,m})$ with $\alpha_{R,m}, \alpha^*_{R,m}, \alpha_{I,m}, \alpha^*_{I,m}$ are the Lagrange multipliers (dual variables) for real and imaginary part of the residuals and $P_m = (m\Delta P)$, $m = 0, \ldots, N_P - 1$ are the pilot positions.

We define the Gram matrix as

$$\mathbf{G}(u, v) = \langle \boldsymbol{\varphi}(P_u), \boldsymbol{\varphi}(P_v) \rangle = K(P_u, P_v) \tag{20}$$

where $K(P_u, P_v)$ is a Mercer's kernel which represent in this paper the RBF kernel matrix which allows obviating the explicit knowledge of the nonlinear mapping $\boldsymbol{\varphi}(\cdot)$. A compact form of the functional problem can be stated in matrix format by placing optimal solution **w** into the primal dual functional and grouping terms. Then, the dual problem consists of maximizing

$$-\frac{1}{2}\boldsymbol{\psi}^H(\mathbf{G} + \gamma\mathbf{I})\boldsymbol{\psi} + \Re(\boldsymbol{\psi}^H Y^P) - (\boldsymbol{\alpha_R} + \boldsymbol{\alpha^*_R} + \boldsymbol{\alpha_I} + \boldsymbol{\alpha^*_I})\mathbf{1}\varepsilon \tag{21}$$

constrained to $0 \le \alpha_{R,m}, \alpha^*_{R,m}, \alpha_{I,m}, \alpha^*_{I,m} \le C$, where $\boldsymbol{\psi} = [\psi_0, \ldots, \psi_{N_P-1}]^T$; $\mathbf{I}$ and $\mathbf{1}$ are the identity matrix and the all-ones column vector, respectively; $\boldsymbol{\alpha_R}$ is the vector which contains the corresponding dual variables, with the other subsets being similarly represented. The weight vector can be obtained by optimizing (21) with respect to $\alpha_{R,m}, \alpha^*_{R,m}, \alpha_{I,m}, \alpha^*_{I,m}$ and then substituting into (19).

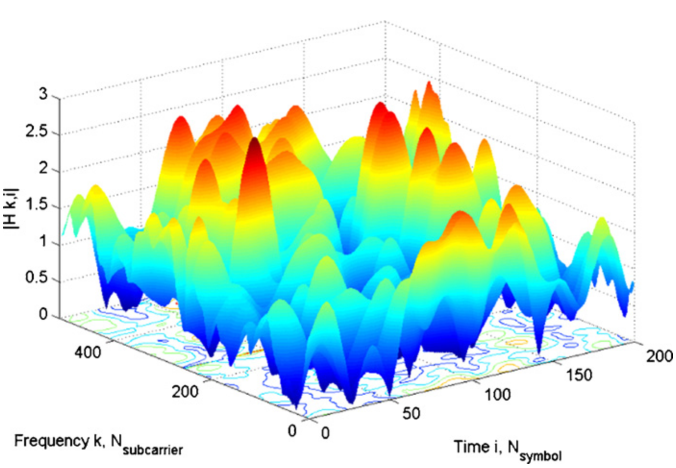

Fig. 1. Variations in time and in frequency of the channel frequency response for mobile speed = 120 km/h.

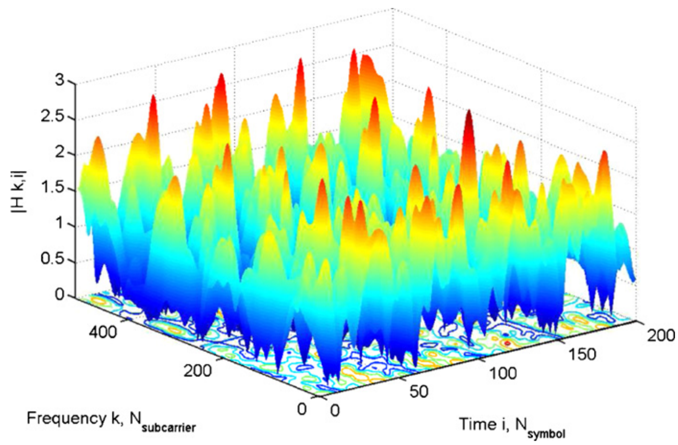

Fig. 2. Variations in time and in frequency of the channel frequency response for mobile speed = 350 km/h.

Therefore, and after training phase, frequency responses at all subcarriers in each OFDM symbol can be obtained by SVM interpolation

$$\hat{H}(k) = \sum_{m=0}^{N_p-1} \psi_m K(P_m, k) + b \tag{22}$$

for $k = 1, \ldots, N$. Note that, the obtained subset of Lagrange multipliers which are nonzero will provide with a sparse solution. As usual in the SVM framework, the free parameter of the kernel and the free parameters of the cost function have to be fixed by some a priori knowledge of the problem, or by using some validation set of observations [5].

5. Simulation results

We consider the channel impulse response of the frequency-selective fading channel model which can be written as

$$h(\tau, t) = \sum_{l=0}^{L-1} h_l(t)\delta(t - \tau_l) \tag{23}$$

where $h_l(t)$ is the impulse response representing the complex attenuation of the lth path, τ_l is the random delay of the lth path and L is the number of multipath replicas. The specification parameters of an extended vehicular A model (EVA) for downlink LTE system with the excess tap delay and the relative power for each path of the channel are shown in Table 1. These parameters are defined by 3GPP standard [7].

Then, we simulate the OFDM downlink LTE system with parameters presented in Table 2. The complex LS-SVM estimate a number of OFDM symbols in the range of 1400 symbols, corresponding to 10 radio frames LTE. Note that, the LTE radio frame duration is 10 ms [8], which is divided into 10 subframes. Each subframe is further divided into two slots, each of.5 ms duration.

In order to test the performance of the nonlinear complex LS-SVM algorithm, two scenarios for downlink LTE system are considered. (Figs. 1 and 2) present the variations in time and in frequency of the channel frequency response for the two scenarios under a mobile speed equal to 120 km/h and 350 km/h, respectively. The complex LS-SVM algorithm parameters are set as: $C = 100$, $\gamma = 10^{-5}$, $\varepsilon = .001$.

The signal to noise ratio (E_s/N_0) is defined as $(E_s/N_0)_{dB} = 10\log_{10}(E|y(n) - w_g(n)|^2/\sigma^2_w)$ [5].

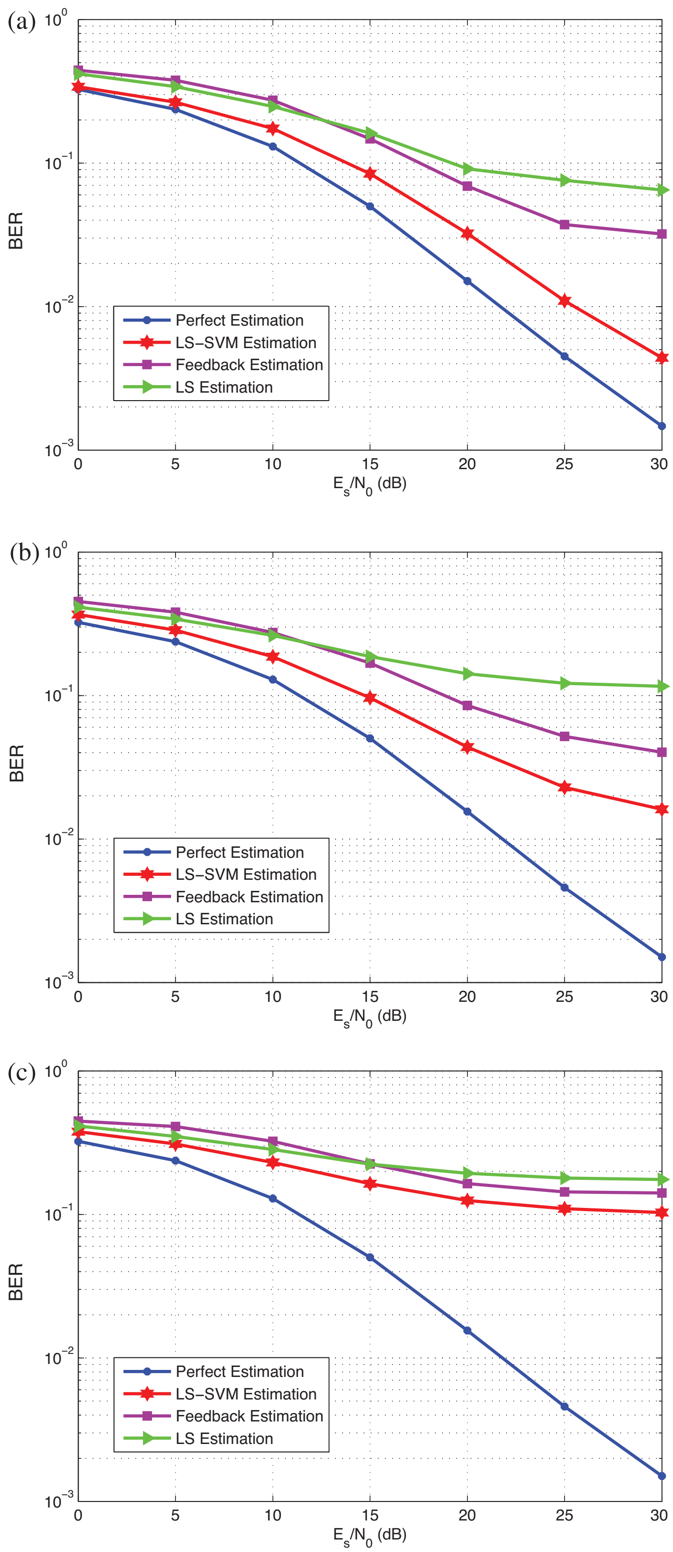

Fig. 3. BER as a function of E_s/N_0 for a mobile speed at 120 km/h with (a) $\Delta P = 6$, (b) $\Delta P = 12$ and (c) $\Delta P = 24$.

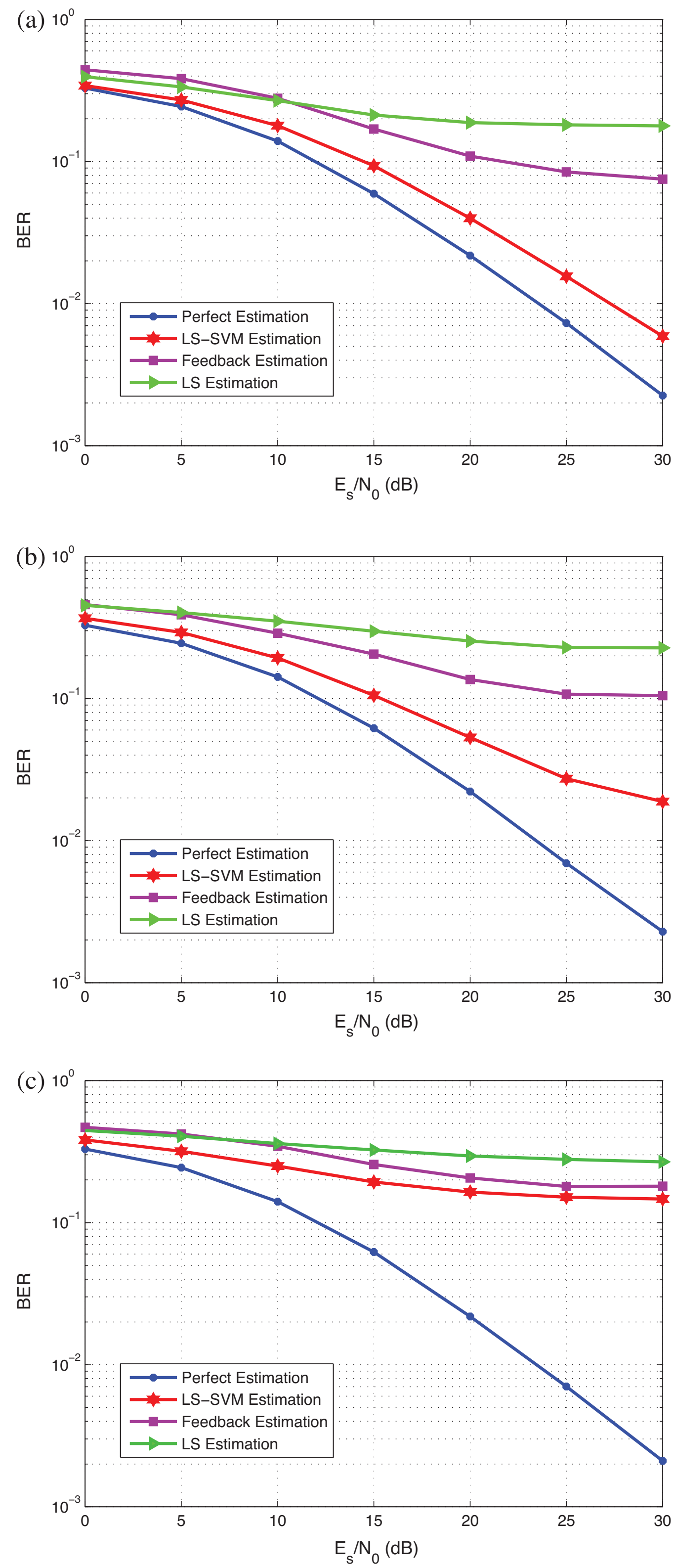

Fig. 4. BER as a function of E_s/N_0 for a mobile speed at 350 km/h with (a) $\Delta P = 6$, (b) $\Delta P = 12$ and (c) $\Delta P = 24$.

Fig. 3 shows the performance of the LS, Decision Feedback and complex LS-SVM algorithms in the presence of additive Gaussian noise as a function of E_s/N_0 for a mobile speed at 120 km/h with different number of pilots. A poor performance is noticeably exhibited by LS in the three different pilot intervals, and good performance is observed with complex LS-SVM which outperforms also Decision Feedback for all noise levels and for all pilot intervals. Fig. 4 present a comparison between LS, Decision Feedback and complex LS-SVM for a mobile speed at 350 km/h which reveals that complex LS-SVM outperforms both estimators LS and Decision Feedback for the different pilot intervals in high mobility conditions.

Table 3
MSE ratios for mobile speed at 120 km/h with (a) $\Delta P = 6$, (b) $\Delta P = 12$ and (c) $\Delta P = 24$.

Method	10 dB	20 dB	30 dB
(a)			
LS (10^{-4})	1.52	.8264	.7571
Feedback (10^{-4})	2.018	.6368	.0626
LS-SVM (10^{-4})	1.123	.1162	.0177
(b)			
LS (10^{-4})	4.264	.9852	.9178
Feedback (10^{-4})	2.059	1.06	.1297
LS-SVM (10^{-4})	1.211	.1629	.0809
(c)			
LS (10^{-4})	5.425	4.057	3.975
Feedback (10^{-4})	4.816	1.464	1.008
LS-SVM (10^{-4})	1.328	.7214	.6698

Table 4
MSE ratios for mobile speed at 350 km/h with (a) $\Delta P = 6$, (b) $\Delta P = 12$ and (c) $\Delta P = 24$.

Method	10 dB	20 dB	30 dB
(a)			
LS (10^{-4})	4.157	1.806	1.709
Feedback (10^{-4})	2.589	.6667	.536
LS-SVM (10^{-4})	1.068	.1226	.0225
(b)			
LS (10^{-4})	4.655	3.247	3.154
Feedback (10^{-4})	3.803	2.897	1.511
LS-SVM (10^{-4})	1.371	.159	.0774
(c)			
LS (10^{-4})	5.863	4.862	4.448
Feedback (10^{-4})	4.054	3.468	3.302
LS-SVM (10^{-4})	1.697	1.198	1.149

MSE (Mean Square Error) of LS, Decision Feedback and complex LS-SVM estimators for a mobile speed at 120 km/h a and 350 km/h for the different cases of pilot interval variations are presented in Tables 3 and 4, respectively. MSE confirms the results obtained for BER (Bit Error Rate) in both scenarios and shows that LS suffers from a high MSE, however, complex LS-SVM performs better than other estimators in different presented cases.

Regarding the complexity of these estimators, LS is the least complex estimator because it contains only one matrix inversion operation. However, the Decision Feedback estimator contains two operations of matrix inversion and two operations of matrix multiplication. On the other hand, the LS-SVM estimator uses quadratic programming (*quadprog* function in Optimization MATLAB Toolbox) with the functions *Buffer* and *kron* for fast computation of kernel matrix using the Kronecker product, and thus the algorithm becomes faster.

6. Conclusion

In this contribution, we have presented a complex LS-SVM based channel estimation technique for a highly selective downlink LTE system. The proposed method is based on learning process that uses training sequence to estimate the channel variations. Our formulation is based on complex LS-SVM specifically developed for pilot-based OFDM systems. Simulations have confirmed the capabilities of the proposed nonlinear complex LS-SVM in the presence of Gaussian noise interfering with the pilot symbols when compared to LS and Decision Feedback methods. The proposal takes into account the temporal-spectral relationship of the OFDM signal for a highly selective channels. The Gram matrix using RBF kernel provides a natural nonlinear extension of the linear LS-SVM which lead to a significant benefit for OFDM communications especially in those scenarios in which deep fading is present.

References

[1] Fernández-Getino García MJ, Rojo-Álvarez JL, Alonso-Atienza F, Martínez-Ramón M. Support vector machines for robust channel estimation in OFDM. IEEE Signal Process J 2006;13(7).
[2] Fernández-Getino García MJ, Páez-Borrallo JM, Zazo S. DFT-based channel estimation in 2D-pilot-symbol-aided OFDM wireless systems. IEEE Veh Technol Conf 2001;2:815–9.
[3] Nanping L, Yuan Y, Kewen X, Zhiwei Z. Study on channel estimation technology in OFDM system. IEEE Comput Soc Conf 2009;77:3–776.
[4] Coleri S, Ergen M, Puri A. Channel estimation techniques based on pilot arrangement in OFDM systems. IEEE Trans Broadcast 2002;48(3):223–9.
[5] Rojo-Álvarez JL, Figuera-Pozuelo C, Martínez-Cruz CE, Camps-Valls G, Alonso-Atienza F, Martínez-Ramón M. Nonuniform interpolation of noisy signals using support vector machines. IEEE Trans Signal Process 2007;55(48):4116–26.
[6] Martínez Ramón M, Xu N, Christodoulou CG. Beamforming Using Support Vector Machines. IEEE Antennas Wireless Propag J 2005;4.
[7] 3rd Generation Partnership Project. Technical specification group radio access network; evolved Universal Terrestrial Radio Access (UTRA): base station (BS) radio transmission and reception. TS 36.104, V8.7.0; September 2009.
[8] 3rd Generation Partnership Project. Technical specification group radio access network; evolved Universal Terrestrial Radio Access (UTRA): physical channels and modulation layer. TS 36.211, V8.8.0; September 2009.
[9] 3rd Generation Partnership Project. Technical specification group radio access network; physical layer aspects for evolved Universal Terrestrial Radio Access (UTRA). TR 25.814, V7.1.0, September 2006.
[10] 3rd Generation Partnership Project. Technical specification group radio access network; evolved Universal Terrestrial Radio Access (UTRA): physical layer procedures. TS 36.213, V8.8.0, September 2009.